ENGINEERING TRANSACTIONS • *Engng. Trans.* • **49**, 4, 537–571, 2001
Polish Academy of Sciences • Institute of Fundamental Technological Research
10.24423/engtrans.542.2001

EVOLUTION OF PLASTIC ANISOTROPY FOR THE POLYCRYSTALLINE MATERIALS IN LARGE DEFORMATION PROCESSES

K. KOWALCZYK

Institute of Fundamental Technological Research
Polish Academy of Sciences
ul. Świętokrzyska 21, 00-049 Warsaw, Poland

Model of evolution of plastic anisotropy due to crystallographic texture development in metals subjected to large deformation processes is presented. The rigid-plastic model of single grain with regularized Schmid law proposed by Gambin is used. Phenomenological and physical descriptions of plastic flow of polycrystals are discussed. Properties of any yield function for orthotropic material subjected to the plane stress state are outlined. Yield conditions of degree m proposed by Hill and Barlat with Lian are analyzed. Finally, phenomenological texture-dependent yield surface is proposed. Evolution of this yield surface is compared with phenomenological yield conditions for two processes: rolling and pure shear.

1. INTRODUCTION

Metal forming processes are associated with large plastic deformation. Large plastic deformation induces evolution of plastic anisotropy of elements. For metals which are polycrystalline materials, induced anisotropy can be caused by several factors such as the change of grain shape and size or crystallographic lattice reorientation. The first factor is called morphological texture development and the second one – crystallographic texture development. Plastic anisotropy caused by crystallographic texture dominates up to moderately large strains [34]. Consequently, to follow evolution of plastic anisotropy in the deformation process texture development should be taken into account in the constitutive equations describing the polycrystal. It is important because evolution of plastic anisotropy can cause many phenomena that influence advantageously or disadvantageously the properties of a metal element. One of the disadvantageous phenomena is for example "earing" observed during deep drawing. Increasing corrosion resistance the gas turbines or increasing fatigue strength of springs used inin the blades of precision equipment belong to advantageous phenomena.

In this paper, the texture development for the initially isotropic grain aggregate will be computed. Rigid-plastic model with isotropic hardening and the regularized Schmid law proposed by GAMBIN in [15, 16], is assumed for the single grain. Anisotropy induced by plastic deformation will be analyzed using a proposed initial yield surface for the polycrystal. In this yield surface, orientation of each grain in the polycrystalline aggregate is taken into account. The proposed texture-dependent yield surface will be compared with the well-known Hill yield surface proposed in 1990 and the Barlat-Lian yield surface proposed in 1989. Principal directions of plastic strain rate will be also obtained from the flow rules associated with the above yield conditions.

2. THE SINGLE GRAIN MODEL

The constitutive model of the single grain presented below is based on the works [28, 29, 1, 2, 16] and [17]. It was applied in the computational program that simulates the change of lattice orientation in the grain in a uniform plastic deformation process.

2.1. Kinematics

Description of kinematical behaviour of the single grain subjected to large elastic-plastic deformation was formulated in the work [28]. It is based on Lee assumption about multiplicative decomposition of the total deformation gradient into the elastic part and the plastic one [37]. Let us distinguish four crystalline solid configurations (Fig. 1): an initial configuration $\mathcal{C}_0$, an intermediate configuration $\mathcal{C}_p$, a reference configuration $\mathcal{C}_r$ and a current configuration $\mathcal{C}_t$. The reference configuration is chosen in such a way that the crystallographic reference frame $\{\mathbf{a}_i\}, i = 1, 2, 3$ is identical with the global reference frame $\{\mathbf{e}_i\}$.

Deformation of the body from the initial configuration to the current configuration is described by the total deformation gradient $\mathbf{F}$:

$$\mathbf{F} = \mathbf{F}^*\mathbf{F}^{\mathbf{P}}, \tag{2.1}$$

where $\mathbf{F}^*$ and $\mathbf{F}^{\mathbf{P}}$ are the elastic part and the plastic part of deformation, respectively. $\mathbf{F}^*$ is given in the configuration $\mathcal{C}_p$ and $\mathbf{F}^{\mathbf{P}}$ is given in the configuration $\mathcal{C}_0$. A deformation gradient that describes mapping of the reference configuration onto the initial configuration can be obtained using a rotation tensor as follows:

$$\mathbf{F}^{\mathbf{0}} = \mathbf{Q}_{\mathbf{0}}^{\mathbf{T}}.$$

$\mathbf{Q_0}$ denotes also the initial orientation of the crystallographic lattice in the global reference frame. Mapping of the reference configuration onto the current config-

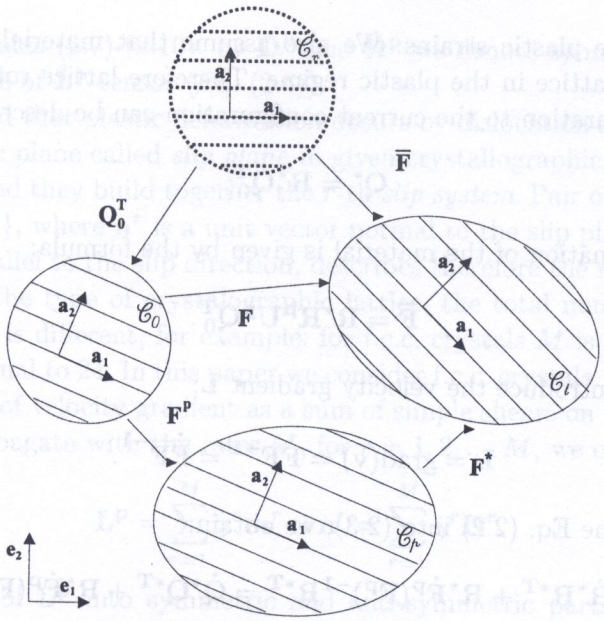

FIG. 1. Decomposition of the deformation gradient $\mathbf{F}$ for the elasto-plastic single crystal.

uration is described by the following deformation gradient:

$$\overline{\mathbf{F}} = \mathbf{F}\mathbf{Q}_0^T.$$

All quantities introduced above depend on the time variable except the tensor $\mathbf{Q}_0$.

It is customary for the single crystal model to assume the global reference frame in such a way that the configurations $\mathcal{C}_r$ and $\mathcal{C}_0$ are identical (see [1] and [2]). Describing crystallographic texture development in some aggregate of the grains we must associate the global reference frame with the polycrystalline sample. This kind of description was also used in [46].

Now, we apply the polar decomposition of the second-rank tensor to the elastic and the plastic parts of the deformation gradient (2.1):

$$\mathbf{F}^* = \mathbf{R}^*\mathbf{U}^*, \quad \mathbf{F}^p = \mathbf{R}^p\mathbf{U}^p,$$

where $\mathbf{R}^*$ and $\mathbf{R}^p$ tensors are rigid rotation tensors while $\mathbf{U}^*$ and $\mathbf{U}^p$ tensors are symmetric and positive defined. The last two tensors are called right stretch tensors.

We limit our considerations to the rigid-plastic model of the single crystal with hardening. In this model we assume that the right elastic stretch tensor $\mathbf{U}^*$ is equal to the identity tensor. This is an appropriate assumption for small

elastic and large plastic strains. We also assume that material *flows* through the motionless lattice in the plastic regime. Therefore lattice rotation from the reference configuration to the current configuration can be described as follows:

$$\mathbf{Q}^* = \mathbf{R}^*\mathbf{Q}_0^{\mathbf{T}},$$

while the deformation of the material is given by the formula:

$$\overline{\mathbf{F}} = \mathbf{R}^*\mathbf{R}^{\mathrm{P}}\mathbf{U}^{\mathrm{P}}\mathbf{Q}_0^{\mathbf{T}}. \tag{2.2}$$

Now let us introduce the velocity gradient $\mathbf{L}$:

$$\mathbf{L} = \mathrm{grad}(\mathbf{v}) = \dot{\mathbf{F}}\mathbf{F}^{-1} = \dot{\overline{\mathbf{F}}}\overline{\mathbf{F}}^{-1}. \tag{2.3}$$

When we put the Eq. (2.2) into (2.3), we obtain:

$$\mathbf{L} = \dot{\mathbf{R}}^*\mathbf{R}^{*\mathbf{T}} + \mathbf{R}^*\dot{\mathbf{F}}^{\mathrm{P}}(\mathbf{F}^{\mathrm{P}})^{-1}\mathbf{R}^{*\mathbf{T}} = \dot{\mathbf{Q}}^*\mathbf{Q}^{*\mathbf{T}} + \mathbf{R}^*\dot{\mathbf{F}}^{\mathrm{P}}(\mathbf{F}^{\mathrm{P}})^{-1}\mathbf{R}^{*\mathbf{T}}. \tag{2.4}$$

The above equation allows us to decompose the velocity gradient into the part associated with the rigid rotation $\mathbf{L}^*$ and the plastic part $\mathbf{L}^{\mathrm{P}}$:

$$\mathbf{L} = \mathbf{L}^* + \mathbf{L}^{\mathrm{P}},$$

where

$$\mathbf{L}^* = \dot{\mathbf{Q}}^*\mathbf{Q}^{*\mathbf{T}}, \tag{2.5}$$

$$\mathbf{L}^{\mathrm{P}} = \mathbf{R}^*\dot{\mathbf{F}}^{\mathrm{P}}(\mathbf{F}^{\mathrm{P}})^{-1}\mathbf{R}^{*\mathbf{T}} = \mathbf{R}^*\hat{\mathbf{L}}^{\mathrm{P}}\mathbf{R}^{*\mathbf{T}}. \tag{2.6}$$

Let us now express $\mathbf{L}$, $\mathbf{L}^*$ and $\mathbf{L}^{\mathrm{P}}$ tensors as follows:

$$\mathbf{L} = \mathbf{D} + \boldsymbol{\Omega}.$$

Tensor $\mathbf{D}$ is the symmetric part of $\mathbf{L}$ and it is called the strain rate tensor. Tensor $\boldsymbol{\Omega}$ is the anti-symmetric part of $\mathbf{L}$ and it is called the spin tensor. We can also decompose $\mathbf{D}$ and $\boldsymbol{\Omega}$ into the part associated with the rigid rotation and the plastic one:

$$\mathbf{D} = \mathbf{D}^{\mathrm{P}} = \frac{1}{2}\mathbf{R}^*\hat{\mathbf{D}}^{\mathrm{P}}\mathbf{R}^{*\mathbf{T}}, \tag{2.7}$$

$$\boldsymbol{\Omega} = \boldsymbol{\Omega}^* + \boldsymbol{\Omega}^{\mathrm{P}}, \tag{2.8}$$

$$\boldsymbol{\Omega}^* = \dot{\mathbf{Q}}^*\mathbf{Q}^{*\mathbf{T}}, \tag{2.9}$$

$$\boldsymbol{\Omega}^{\mathrm{P}} = \frac{1}{2}\mathbf{R}^*\hat{\boldsymbol{\Omega}}^{\mathrm{P}}\mathbf{R}^{*\mathbf{T}}. \tag{2.10}$$

In the formulas (2.7)-(2.10), by $\hat{\mathbf{D}}^{\mathbf{P}}$ and $\hat{\mathbf{\Omega}}^{\mathbf{P}}$ we denote symmetric and anti-symmetric parts of $\hat{\mathbf{L}}^{\mathbf{P}}$ tensor (Eq. (2.6)).

It is assumed that plastic deformation occurs by dislocation slip on the given crystallographic plane called *slip plane* in given crystallographic direction called *slip direction* and they build together the r-th *slip system*. Pair of the orthogonal vectors $\{\mathbf{m}^r, \mathbf{n}^r\}$, where $\mathbf{n}^r$ is a unit vector normal to the slip plane and $\mathbf{m}^r$ is a unit vector parallel to the slip direction, describes therefore the r-th slip system. Depending on the type of crystalographic lattice, the total number of possible slip systems M is different, for example: for f.c.c. crystals M is equal to 12 and for b.c.c. it is equal to 24. In this paper we consider f.c.c. crystals. We can define a plastic part $\mathbf{L}^{\mathbf{P}}$ of velocity gradient as a sum of simple shears on all slip systems. When they propagate with the rates $\dot{\gamma}^r$, for $r = 1, 2, ..., M$, we obtain:

$$\mathbf{L}^{\mathbf{P}} = \sum_{r=1}^{M} \dot{\gamma}^r \mathbf{m}^r \otimes \mathbf{n}^r = \sum_{r=1}^{M} \dot{\gamma}^r \mathbf{D}^r.$$

Decomposition of $\mathbf{L}^{\mathbf{P}}$ into symmetric and anti-symmetric parts looks then as follows:

$$\mathbf{L}^{\mathbf{P}} = \mathbf{D}^{\mathbf{P}} + \mathbf{\Omega}^{\mathbf{P}} = \sum_{r=1}^{M} \dot{\gamma}^r \mathbf{P}^r + \sum_{r=1}^{M} \dot{\gamma}^r \mathbf{W}^r, \tag{2.11}$$

where $\mathbf{P}^r$ and $\mathbf{W}^r$ are symmetric and anti-symmetric parts of $\mathbf{m}^r \otimes \mathbf{n}^r$ diad, respectively. It is worth noting that because of orthogonality of $\mathbf{m}^r$ and $\mathbf{n}^r$ vectors, tensor $\mathbf{D}^{\mathbf{P}}$ is deviator.

$\mathbf{P}^r$ and $\mathbf{W}^r$ tensors change during the deformation process due to rotation of the lattice directions $\mathbf{m}^r$ and $\mathbf{n}^r$. Evolution of these directions can be described by the formulas:

$$\dot{\mathbf{m}}^r = \mathbf{\Omega}^* \mathbf{m}^r, \quad \dot{\mathbf{n}}^r = \mathbf{\Omega}^* \mathbf{n}^r.$$

When we want to calculate the texture evolution, we look for the lattice orientation at the time $t + \Delta t$ having its orientation at the time t. We describe the lattice orientation by three Euler angles $\{\varphi_i\}$ that define the rotation tensor $\mathbf{Q}^*$. Evolution of these angles can be calculated from the equations:

$$\varphi_i^{t+\Delta t} = \varphi_i^t + \dot{\varphi}_i \Delta t, \quad i = 1, 2, 3.$$

To find the rates of the Euler angles $\dot{\varphi}_i$ we apply the rule obtained by Clement [12]. This rule uses the formula (2.9) in the form:

$$\dot{\mathbf{Q}}^* = \mathbf{\Omega}^* \mathbf{Q}^*.$$

When we express the rotation tensor $\mathbf{Q}^*$ by the Euler angles φ_i^t, we can obtain their rates $\dot{\varphi}_i^t$:

$$\dot{\varphi}_1 = \omega_{12}^* - \frac{1}{\tan\varphi_2^t}(\sin\varphi_1^t\omega_{23}^* - \cos\varphi_1^t\omega_{13}^*), \tag{2.12}$$

$$\dot{\varphi}_2 = \sin\varphi_1^t\omega_{13}^* + \cos\varphi_1^t\omega_{23}^*, \tag{2.13}$$

$$\dot{\varphi}_3 = -\frac{\cos\varphi_1^t}{\sin\varphi_2^t}\omega_{12}^* + \frac{\sin\varphi_1^t}{\sin\varphi_2^t}\omega_{23}^*, \tag{2.14}$$

where ω_{ij}^* are the components of the spin tensor $\boldsymbol{\Omega}^*$. These equations are well defined when $\varphi_2^t \neq 0$. When $\varphi_2^t = 0$ we must apply the following equations:

$$\dot{\psi} = \omega_{12}^*, \quad \text{where } \psi = \varphi_1^t + \varphi_3^t, \tag{2.15}$$

$$\dot{\varphi}_2 = \begin{cases} \dfrac{\omega_{23}^*}{\cos\tilde{\varphi}_1} & \text{where } \tilde{\varphi}_1 = \arctan\dfrac{\omega_{13}^*}{\omega_{23}^*} \quad \text{for } \omega_{23}^* \neq 0 \\ \omega_{13}^* & \text{where } \tilde{\varphi}_1 = \dfrac{\pi}{2} \quad \text{for } \omega_{23}^* = 0 \end{cases}. \tag{2.16}$$

In this case the Euler angles at the time $t + \Delta t$ can be calculated as follows:

$$\begin{aligned} \varphi_1^{t+\Delta t} &= \tilde{\varphi}_1 + \dot{\psi}\Delta t, \\ \varphi_2^{t+\Delta t} &= \dot{\varphi}_2\Delta t, \\ \varphi_3^{t+\Delta t} &= \tilde{\varphi}_3, \quad \text{where} \quad \tilde{\varphi}_3 = \psi - \tilde{\varphi}_1. \end{aligned}$$

The lattice spin $\boldsymbol{\Omega}^*$ that occurs in the above equations can be determined as a difference between the total spin $\boldsymbol{\Omega}$ and the plastic spin $\boldsymbol{\Omega}^{\mathrm{p}}$. Assuming that the total spin is given by the boundary conditions, the plastic spin has to be calculated from additional constitutive equation.

2.2. *Constitutive laws*

In the models of single crystal plasticity the Schmid law is used. It says that the plastic flow on the r-th slip system begins when the resolved shear stress τ^r on this system reaches the critical value τ_{c}^r which is the material constant. Therefore

$$\gamma^r \neq 0 \Longrightarrow \tau^r = \tau_{\mathrm{c}}^r. \tag{2.17}$$

The resolved shear stress τ^r is calculated as a projection of the Kirchhoff stress tensor $\boldsymbol{\tau}$ on the slip plane and the slip direction:

$$\tau^r = \mathbf{m}^r : \boldsymbol{\tau} : \mathbf{n}^r = \boldsymbol{\tau} : \mathbf{D}^r, \tag{2.18}$$

where ":" denotes the full product of tensors. The set of slip systems in which the total work done during slipping is minimal, is chosen from all possible combinations. In the models that use the Schmid law as a yield condition, the problem of non-unique selection of active slip systems exists.

To overcome this difficulty GAMBIN [16, 17] has proposed the model of interacting slip systems. The shear rate $\dot{\gamma}^r$ can be associated with the resolved shear stress τ^r by the empirical relationship between the mean velocity of dislocation on the r-th slip system and the resolved shear stress as well as between the shear rate and the mean velocity of dislocation [31]. Finally, these relationships lead to the equation:

$$\dot{\gamma}^r = \lambda \frac{(\tau^r)^{2n-1}}{(\tau_c^r)^{2n}}. \tag{2.19}$$

The coefficient λ is identical for all slip system. Slips with different rates $\dot{\gamma}^r$ described by the formula (2.19) appear on all slip systems simultaneously. It is worth noting that when the exponent n increases, the perceptible slip occurs only on those systems for which the Schmid condition (2.17) is satisfied.

Putting the Eq. (2.19) into the formula (2.11) that describe $\mathbf{D^p}$ and $\mathbf{\Omega^p}$ we obtain:

$$\mathbf{D^p} = \lambda \sum_{r=1}^{M} \frac{1}{\tau_c^r} \left(\frac{\tau^r}{\tau_c^r} \right)^{2n-1} \mathbf{P^r},$$

$$\mathbf{\Omega^p} = \lambda \sum_{r=1}^{M} \frac{1}{\tau_c^r} \left(\frac{\tau^r}{\tau_c^r} \right)^{2n-1} \mathbf{W^r}.$$

The above equations can be treated as flow rules associated with the following plastic potential:

$$F(\boldsymbol{\tau}, \varphi_k) = \frac{1}{2n} \left(\sum_{r=1}^{M} \left(\frac{\tau^r}{\tau_c^r} \right)^{2n} - m \right), \quad \text{where} \quad \tau^r = \boldsymbol{\tau} : \mathbf{D}^r. \tag{2.20}$$

A dimensionless constant m is a lattice orientation independent quantity. A smooth yield condition is connected with the potential (2.20). It has the form:

$$\sum_{r=1}^{M} \left(\frac{\tau^r}{\tau_c^r} \right)^{2n} = m,$$

where the exponent $n > 1$ is some dimensionless material parameter.

We can assume that the critical shear stress τ_c^r is constant during the deformation process or we can introduce a hardening rule that specifies the evolution of τ_c^r. In our calculations we use the following hardening law [1]:

$$\dot{\tau_c^r} = \sum_{q=1}^{M} h_{rq} \dot{\gamma}^r.$$

Coefficients h_{rq} are the components of the matrix of hardening moduli H and:

$$h_{rq} = \begin{cases} h_1 & \text{for } r = q \\ h_2 > h_1 & \text{for } r \neq q \end{cases}.$$

In this case we have the latent hardening ($h_2 > h_1$) for non-active slip systems for which $\tau^r < \tau_c^r$.

Model of texture development due to the plastic flow in the aggregate of the grains presented in this paper is based on the described constitutive model for the single grain.

3. Yield surfaces for polycrystals

We can divide the yield conditions for the metal polycrystals into: *phenomenological* that are based on the classical theory of plasticity, and *physical* ones that use the knowledge about microstructure of the polycrystals. The first conditions are proposed with the assumption that the polycrystalline material is homogeneous at the macro-level and a yield surface depends on macroscopic stress and strain measures as well as their rates. The second ones use the information about yielding of the grains that build the polycrystalline aggregate.

3.1. Phenomenological yield conditions for metals

Usually phenomenological yield conditions are given by the scalar function of the stress tensor, the strain tensor or its plastic part as well as the material derivatives of those tensors and the parameters that describe anisotropy of the material. In most of the theories it is assumed that this function depends only on the stress tensor and the material parameters, which means that $f = f(\boldsymbol{\sigma})$ and the yield condition takes the form:

$$f(\boldsymbol{\sigma}) = (\sigma_o)^m. \tag{3.1}$$

Equation (3.1) describes a surface that encloses the class of stress states in the stress space for which deformation of the polycrystal is only elastic. This class is given by the inequality:

$$f(\boldsymbol{\sigma}) < (\sigma_o)^m, \tag{3.2}$$

where σ_o and the exponent m are some material parametrs. This surface is called the yield surface. According to the basic theory of the constitutive Eqs. [28, 29], the yield surface should be convex and in the large strain theory the strain rate tensor $\mathbf{D}^{\mathrm{P}}$ or in the small strain theory the tensor $\dot{\boldsymbol{\varepsilon}}^{\mathrm{P}}$ should be normal to this

surface. Moreover, it is often assumed that the yield function f is homogeneous. Thus we can write the following relationships (see [27]):

$$\mathbf{D}^{\mathrm{P}} = \lambda \frac{\partial f}{\partial \boldsymbol{\sigma}} \tag{3.3}$$

for some positive scalar λ due to normality of the flow rule, and

$$f(\mu\boldsymbol{\sigma}) = \mu^m f(\boldsymbol{\sigma}), \quad \boldsymbol{\sigma} : \frac{\partial f}{\partial \boldsymbol{\sigma}} = m f(\boldsymbol{\sigma}) \tag{3.4}$$

for any scalar $\mu > 0$ due to homogeneity of degree m of the yield function f.

In most cases it is also assumed for metals that plastic flow does not occur for any hydrostatic stress state. Moreover, the value of the yield stress is equal for the stress states that differ from each other only by their signs.

One of the first yield conditions for any anisotropic material is the von Mises criterion proposed in 1928. It is defined by the quadratic function of the stress components [39]. A special case of this yield function is the well-known Hill condition for the orthotropic materials proposed in 1948 [22, 23]. Thorough analysis of this yield surface can be found in the paper [33]. Energetic interpretation of the quadratic yield conditions for the anisotropic materials was given in [40, 41] and [43].

Observations of metal forming processes and phenomena that took place during utilization of the formed elements proved that the quadratic yield function was insufficient to describe a lot of aspects related with the plastic flow of the material such as "earing" that took place during sheet drawing, increasing corrosion resistance in the blades of the gas turbines or increasing fatigue strength of springs used in the precision equipment. The yield surfaces of higher degree were searched. The Gotoh criterion proposed in 1977 using the tensorial polynomial of degree four was among them [20]. This yield condition was formulated for the orthotropic material subjected to the plane stress state. The other one was the Hill yield condition of degree m formulated in 1979 [26]. It could be used for the stress states that were co-axial with the main axes of orthotropy. The yield function was described by seven material parameters that should be derived from experiments, which was rather troublesome. The author suggested that one could assume some of these parameters to be equal to zero, without loosing the ability to describe the phenomena that could not be taken into account by his quadratic yield condition. Hill outlined four special cases of his new yield function in the case of plane isotropy (the sheet is isotropic in its plane) and plane stress state. In 1990 one of these special cases was re-formulated to encompass any orthotropic sheet subjected to the plane stress state [27]. Another orthotropic yield surface of degree m, widely used nowadays for the metal sheets, was given by BARLAT and LIAN in 1989 [5]. At first it was formulated for the plane stress state and in 1991 it was extended to any stress state [6].

As it has been already mentioned, in the majority of cases, the yield function depends on the tensor $\boldsymbol{\sigma}$ and the material parameters. In order to describe the change of the yield surface due to plastic deformation one must use the yield function that depends on the plastic strain or the plastic strain rate apart from the stress tensor. It can be done in two ways: one can use the function that depends on these quantities directly, which means that $f = f(\boldsymbol{\sigma}, \mathbf{D}^p)$ or one can use the function where the material parameters depend on these quantities.

Below we will consider the Hill yield condition proposed in 1990 and the Barlat-Lian yield condition formulated in 1989. They both refer to the plane stress state, so now we outline general properties of the function describing the yield condition for the orthotropic material in two-dimensional space.

The form of the yield function that does not depend on the choice of the reference system is useful in the analysis. Such a form of yield function one can find using the theory of representation of the anisotropic tensor functions formulated by BOEHLER [9, 10] (see also [32]). According to this theory, the orthotropic scalar function of the tensor $\boldsymbol{\sigma}$ in two-dimensional space has the form:

$$f(\boldsymbol{\sigma}) = f_1(\operatorname{tr}\boldsymbol{\sigma}, \operatorname{tr}\boldsymbol{\sigma}^2, \operatorname{tr}\mathbf{M}\boldsymbol{\sigma}), \tag{3.5}$$

where "tr" denotes trace of the tensor and $\mathbf{M} = \mathbf{m} \otimes \mathbf{m}$ and $\mathbf{m}$ is the unit vector co-axial with one of the main directions of orthotropy. The three invariants in the Eq. (3.5) can be expressed by components $\sigma_{\alpha\beta}$ of the plane stress tensor in the basis co-axial with orthotropy as follows:

$$\operatorname{tr}\boldsymbol{\sigma} = \sigma_{11} + \sigma_{22}, \quad \operatorname{tr}\boldsymbol{\sigma}^2 = \sigma_{11}^2 + \sigma_{22}^2 + 2\sigma_{12}^2, \quad \operatorname{tr}\mathbf{M}\boldsymbol{\sigma} = \sigma_{11}. \tag{3.6}$$

Three invariants from the Eq. (3.5) can be replaced by another equivalent set of invariants, for example: $\{\operatorname{tr}\boldsymbol{\sigma}, \operatorname{tr}\mathbf{s}^2, \operatorname{tr}\mathbf{M}\mathbf{s}\}$, where $\mathbf{s}$ is the plane stress deviator: $\mathbf{s} = \boldsymbol{\sigma} - \frac{1}{2}(\operatorname{tr}\boldsymbol{\sigma})\mathbf{I}$ and $\mathbf{I}$ is the identity tensor in two-dimensional space. In this case, function f takes the form:

$$f(\boldsymbol{\sigma}) = f_2(\operatorname{tr}\boldsymbol{\sigma}, \operatorname{tr}\mathbf{s}^2, \operatorname{tr}\mathbf{M}\mathbf{s}) \tag{3.7}$$

and the invariants of the stress deviator $\mathbf{s}$ are expressed by the components $\sigma_{\alpha\beta}$ as follows:

$$\operatorname{tr}\mathbf{s}^2 = \frac{1}{2}(\sigma_{11} - \sigma_{22})^2 + 2\sigma_{12}^2, \quad \operatorname{tr}\mathbf{M}\mathbf{s} = \frac{1}{2}(\sigma_{11} - \sigma_{22}). \tag{3.8}$$

The plane components of the plastic strain rate tensor can be obtained using the invariant form of the yield function f (3.7) in the flow rule (3.3). The Eq. (3.3) takes the form:

$$\mathbf{D}^{\mathbf{p}} = \lambda \left[g_1(\boldsymbol{\sigma})\mathbf{I} + 2g_2(\boldsymbol{\sigma})\mathbf{s} + g_3(\boldsymbol{\sigma})(\mathbf{M} - \frac{1}{2}\mathbf{I}) \right], \tag{3.9}$$

where functions $g_i(\boldsymbol{\sigma})$ are the scalar orthotropic functions of the stress tensor such as:

$$g_1 = \frac{\partial f}{\partial \mathrm{tr}\,\boldsymbol{\sigma}}, \quad g_2 = \frac{\partial f}{\partial \mathrm{tr}\,\mathbf{s}^2}, \quad g_3 = \frac{\partial f}{\partial \mathrm{tr}\,\mathbf{Ms}}.$$

The functions g_1 and g_3 are homogeneous of degree $m-1$, and the function g_2 is homogeneous of degree $m-2$. Moreover, additional non-zero component of the tensor $\mathbf{D^p}$ in three-dimensional space can be obtained from the assumption that $\mathbf{D^p}$ tensor is deviatoric:

$$D^{\mathrm{p}}_{33} = -(D^{\mathrm{p}}_{11} + D^{\mathrm{p}}_{22}). \tag{3.10}$$

Note that because the yield function f is homogeneous of degree m (Eq. (3.4)), the following equation is fulfilled:

$$g_1 \mathrm{tr}\,\boldsymbol{\sigma} + 2g_2 \mathrm{tr}\,\mathbf{s}^2 + g_3 \mathrm{tr}\,\mathbf{Ms} = m\sigma_o^m. \tag{3.11}$$

The tensile (or compression) yield stress at any orientation ϕ to one of the orthotropy axes, for example co-axial with the vector $\mathbf{m}$ (see Fig. 2), is often used in the analysis of material anisotropy. Then the stress tensor can be expressed as follows:

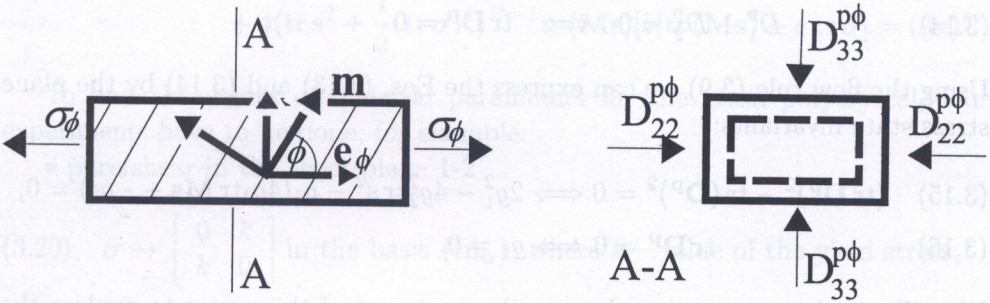

FIG. 2. Uniaxial tension of the sample for the orthotropic material.

$$\boldsymbol{\sigma} = \sigma_\phi \mathbf{e}_\phi \otimes \mathbf{e}_\phi = \sigma_\phi \mathbf{W}_\phi,$$

where $\mathbf{e}_\phi$ is the unit vector that describes the tensile direction. When we substitute the stress tensor into the Eqs. (3.5) or (3.7) we obtain:

$$f(\sigma_\phi \mathbf{W}_\phi) = \sigma_\phi^m f(\mathbf{W}_\phi) = \sigma_\phi^m f_1(1, 1, \cos^2\phi) = \sigma_\phi^m f_2(1, \frac{1}{2}, \frac{1}{2}\cos 2\phi).$$

Together with the yield condition (3.1) it gives the following expression:

$$\left(\frac{\sigma_o}{\sigma_\phi}\right)^m = f_1(1, 1, \cos^2\phi) = f_2(1, \frac{1}{2}, \frac{1}{2}\cos 2\phi).$$

Formulas (3.9), (3.10) and (3.11) enable us to determine the dependence that describe the Lankford coefficient R_ϕ for the orthotropic material under tension in the direction established by the angle ϕ to the versor $\mathbf{m}$. This coefficient is defined as a ratio: (in-plane transverse rate of plastic deformation)/(through-thickness rate of plastic deformation), so

$$R_\phi = \frac{D_{22}^{p\phi}}{D_{33}^{p\phi}} = \frac{m}{2g_1(\mathbf{W}_\phi)} \left(\frac{\sigma_o}{\sigma_\phi}\right)^m - 1. \tag{3.12}$$

Metal forming is limited by the strain localization phenomena. The stress states, which give eigenvalues of the tensor $\mathbf{D}^p$ in three-dimensional space equal to zero, can cause strain localization ([27, 4, 38]). At least one eigenvalue of $\mathbf{D}^p$ tensor is equal to zero when:

$$D_1^p D_2^p = 0 \quad \text{or} \quad D_1^p + D_2^p = 0.$$

These conditions can be formulated by the invariants of $\mathbf{D}^p$ in two-dimensional space as follows:

$$D_1^p D_2^p = 0 \iff (\operatorname{tr} \mathbf{D}^p)^2 - \operatorname{tr} (\mathbf{D}^p)^2 = 0, \tag{3.13}$$

$$D_1^p + D_2^p = 0 \iff \operatorname{tr} \mathbf{D}^p = 0. \tag{3.14}$$

Using the flow rule (3.9) we can express the Eqs. (3.13) and (3.14) by the plane stress state invariants:

$$(\operatorname{tr} \mathbf{D}^p)^2 - \operatorname{tr} (\mathbf{D}^p)^2 = 0 \iff 2g_1^2 - 4g_2^2 \operatorname{tr} \mathbf{s}^2 - g_3(4g_2 \operatorname{tr} \mathbf{Ms} + \frac{1}{2} g_3) = 0, \tag{3.15}$$

$$\operatorname{tr} \mathbf{D}^p = 0 \iff g_1 = 0. \tag{3.16}$$

We will use these two expressions in the next part of this paper to explore the anisotropy evolution for the prescribed path of plastic deformation.

3.1.1. The Hill yield condition 1990. The Hill yield condition was proposed in 1990 [27] in the following form:

$$f_H(\boldsymbol{\sigma}) = |\sigma_{11} + \sigma_{22}|^m + \left(\frac{\sigma}{\tau}\right)^m [(\sigma_{11} - \sigma_{22})^2 + 4\sigma_{12}^2]^{\frac{m}{2}} + (\sigma_{11}^2 + \sigma_{22}^2 + 2\sigma_{12}^2)^{\frac{m}{2}-1} [-2a(\sigma_{11}^2 - \sigma_{22}^2) + b(\sigma_{11} - \sigma_{22})^2] = (2\sigma)^m, \tag{3.17}$$

where $\sigma_{\alpha\beta}$ are the stress tensor $\boldsymbol{\sigma}$ components in the basis $\{\mathbf{m}_\alpha, \alpha = 1, 2\}$ associated with the main directions of orthotropy in the sheet plane. Note that the function f_H is homogeneous of degree m. In the criterion (3.17), σ, τ, a, b, m are the material parameters that have to be identified in experiments. They do

not change their value during the whole plastic deformation process for the rigid ideally plastic material. In the case of isotropic hardening it is assumed that the parameter σ is a function of plastic strain while the ratio of this parameter to the other remains constant during the process. The yield surface preserves its shape and varies only in its size. If we introduce a different evolution law for each material parameter, we will be able to obtain anisotropic hardening and describe the evolution of plastic anisotropy of given material. Author suggests the exponent m to be less than 2. If $m = 2$, then from the Eq. (3.17) we will obtain the Hill yield condition proposed in 1948.

Using the Eq. (3.6) in (3.17), the Hill yield function takes the form:

$$f_1^{\mathrm{H}} = |\operatorname{tr}\boldsymbol{\sigma}|^m + \left(\frac{\sigma}{\tau}\right)^m [2\operatorname{tr}\boldsymbol{\sigma}^2 - (\operatorname{tr}\boldsymbol{\sigma})^2]^{\frac{m}{2}} + 4(\operatorname{tr}\boldsymbol{\sigma}^2)^{\frac{m}{2}-1}(\operatorname{tr}\mathbf{M}\boldsymbol{\sigma} - \frac{1}{2}(\operatorname{tr}\boldsymbol{\sigma}))[b(\operatorname{tr}\mathbf{M}\boldsymbol{\sigma} - \frac{1}{2}(\operatorname{tr}\boldsymbol{\sigma})) - a\operatorname{tr}\boldsymbol{\sigma}] = (2\sigma)^m, \tag{3.18}$$

while in the basis of the deviator invariants (3.8):

$$f_2^{\mathrm{H}} = |\operatorname{tr}\boldsymbol{\sigma}|^m + \left(\frac{\sigma}{\tau}\right)^m [2\operatorname{tr}\mathbf{s}^2]^{\frac{m}{2}} + 4(\operatorname{tr}\mathbf{s}^2 + \frac{1}{2}(\operatorname{tr}\boldsymbol{\sigma})^2)^{\frac{m}{2}-1}\operatorname{tr}(\mathbf{Ms})[b(\operatorname{tr}(\mathbf{Ms}) - a\operatorname{tr}\boldsymbol{\sigma}] = (2\sigma)^m. \tag{3.19}$$

To find the values of material parameters for the given polycrystal, four experiments have to be done, for example:

- pure shear in the sheet plane 1-2

$$\boldsymbol{\sigma} \to \begin{bmatrix} 0 & k \\ k & 0 \end{bmatrix} \text{ in the basis } \{\mathbf{m}_\alpha\}, \text{ where } k \text{ – value of the yield stress;} \tag{3.20}$$

- equibiaxial tension in the sheet plane 1-2

$$\boldsymbol{\sigma} \to \begin{bmatrix} Y_p & 0 \\ 0 & Y_p \end{bmatrix} \text{ in the basis } \{\mathbf{m}_\alpha\}, \text{ where } Y_p \text{ – value of the yield stress;} \tag{3.21}$$

- uniaxial tension along the $\mathbf{m}_1$ direction

$$\boldsymbol{\sigma} \to \begin{bmatrix} Y_1 & 0 \\ 0 & 0 \end{bmatrix} \text{ in the basis } \{\mathbf{m}_\alpha\}, \text{ where } Y_1 \text{ – value of the yield stress;} \tag{3.22}$$

- uniaxial tension along the $\mathbf{m}_2$ direction

$$\boldsymbol{\sigma} \to \begin{bmatrix} 0 & 0 \\ 0 & Y_2 \end{bmatrix} \text{ in the basis } \{\mathbf{m}_\alpha\}, \text{ where } Y_2 \text{ – value of the yield stress.} \tag{3.23}$$

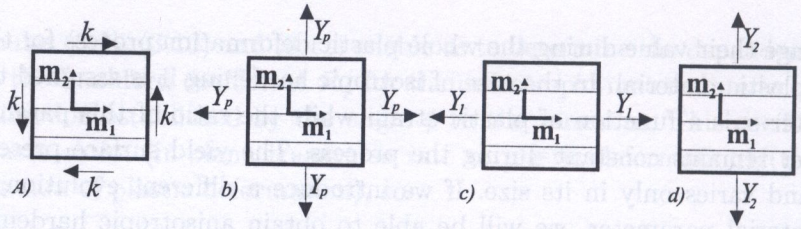

FIG. 3. Experiments proposed to establish material parameters that define the Hill yield condition: a) pure shear, b) equi-biaxial tension, c) uniaxial tension in $\mathbf{m}_1$ direction, d) uniaxial tension in $\mathbf{m}_2$ direction.

Scheme of these experiments is presented in the Fig. 3. When we substitute values of the yield stresses (3.20)-(3.23) in the Eqs. (3.18) or (3.19), we have the following expressions for the parameters that define the Hill yield condition (3.17):

$$a = \tfrac{1}{4}\left[\left(\frac{2Y_p}{Y_2}\right)^m - \left(\frac{2Y_p}{Y_1}\right)^m\right], \quad b = \tfrac{1}{2}\left[\left(\frac{2Y_p}{Y_1}\right)^m + \left(\frac{2Y_p}{Y_2}\right)^m\right] - \left(\frac{Y_p}{k}\right)^m - 1, \tag{3.24}$$

$$\sigma = Y_p, \qquad \tau = k.$$

Hill gives other possible tests that can serve to find the value of the parameter b: uniaxial tension or pure shear at $\phi = 45^o$ to the $\mathbf{m}_1$ axis in the sheet plane. Denoting the values of the yield stresses in these tests by Y_{45} and τ_{45}, respectively, we obtain the following expressions for the parameter b:

$$b = \frac{1}{2}\left[\left(\frac{2Y_p}{Y_1}\right)^m + \left(\frac{2Y_p}{Y_2}\right)^m\right] - \left(\frac{2Y_p}{Y_{45}}\right)^m = 2^{\frac{m}{2}-1}\left[\left(\frac{Y_p}{\tau_{45}}\right)^m - \left(\frac{Y_p}{\tau}\right)^m\right]. \tag{3.25}$$

Let us consider the form taken by the discussed yield function in special cases of orthotropy. For cubic symmetry we have:

$$Y_1 = Y_2 = Y \Rightarrow a = 0$$

and the yield condition in the invariant form (3.19) is reduced to:

$$|\operatorname{tr}\boldsymbol{\sigma}|^m + \left(\frac{\sigma}{\tau}\right)^m [2\operatorname{tr}\mathbf{s}^2]^{\frac{m}{2}} + 4(\operatorname{tr}\mathbf{s}^2 + \frac{1}{2}(\operatorname{tr}\boldsymbol{\sigma})^2)^{\frac{m}{2}-1}[b\operatorname{tr}(\mathbf{Ms})]^2 = (2\sigma)^m.$$

If the material is isotropic in the sheet plane, material properties do not depend on tensor $\mathbf{M}$, so $b = 0$ and therefore:

$$|\operatorname{tr}\boldsymbol{\sigma}|^m + \left(\frac{\sigma}{\tau}\right)^m [2\operatorname{tr}\mathbf{s}^2]^{\frac{m}{2}} = (2\sigma)^m. \tag{3.26}$$

If we express the invariants appearing in this equation by the principal components of plane stress tensor $\boldsymbol{\sigma}$, we obtain one of the four special cases of the Hill yield criterion proposed in 1979 [26].

The tensile (or compression) yield stress in the sheet plane at the angle ϕ to one of the orthotropy axis, for example $\mathbf{m}_1$, predicted by the analyzed yield criterion is given by the formula:

$$\sigma_\phi = \pm \left[\frac{(2\sigma)^m}{1 + \left(\frac{\sigma}{\tau}\right)^m + \cos 2\phi (b \cos 2\phi - 2a)} \right]^{\frac{1}{m}}. \tag{3.27}$$

In the case of Hill yield function $f_{\mathrm{H}}(\boldsymbol{\sigma})$ we obtain the following expressions that define the functions g_i appearing in the flow rule (3.9):

$$\begin{aligned} g_1 = {} & m|\operatorname{tr}\boldsymbol{\sigma}|^{m-1}\operatorname{sgn}(\operatorname{tr}\boldsymbol{\sigma}) \\ & + 2(\operatorname{tr}\mathbf{s}^2 + \frac{1}{2}(\operatorname{tr}\boldsymbol{\sigma})^2)^{\frac{m}{2}-2}\operatorname{tr}\mathbf{Ms}[b(m-2)\operatorname{tr}\mathbf{Mstr}\,\boldsymbol{\sigma} \\ & - a((m-1)(\operatorname{tr}\boldsymbol{\sigma})^2 + 2\operatorname{tr}\mathbf{s}^2)], \end{aligned} \tag{3.28}$$

$$\begin{aligned} g_2 = {} & m\left(\frac{\sigma}{\tau}\right)^m (2\operatorname{tr}\mathbf{s}^2)^{\frac{m}{2}-1} \\ & + (2m-4)(\operatorname{tr}\mathbf{s}^2 + \frac{1}{2}(\operatorname{tr}\boldsymbol{\sigma})^2)^{\frac{m}{2}-2}\operatorname{tr}\mathbf{Ms}(b\operatorname{tr}\mathbf{Ms} - a\operatorname{tr}\boldsymbol{\sigma}), \end{aligned} \tag{3.29}$$

$$g_3 = 4(\operatorname{tr}\mathbf{s}^2 + \frac{1}{2}(\operatorname{tr}\boldsymbol{\sigma})^2)^{\frac{m}{2}-1}(2b\operatorname{tr}\mathbf{Ms} - a\operatorname{tr}\boldsymbol{\sigma}). \tag{3.30}$$

Substituting the Eqs. (3.27) and (3.28) into (3.12) we can determine formulas that give the Lankford coefficient R_ϕ for the material that is described by the considered yield condition:

$$R_\phi = \frac{D_{22}^{\mathrm{p}\phi}}{D_{33}^{\mathrm{p}\phi}} = \frac{-1 + \left(\frac{\sigma}{\tau}\right)^m + \frac{2}{m}b(\cos 2\phi)^2}{2 - 2a\cos 2\phi + \frac{m-2}{m}b(\cos 2\phi)^2}. \tag{3.31}$$

3.1.2. The Barlat-Lian yield condition 1989. In 1989 Barlat and Lian proposed another yield condition of degree m for the polycrystalline materials and the plane stress state [5]. It has the following form in the stress $\boldsymbol{\sigma}$ components in the basis $\{\mathbf{m}_\alpha\}$ associated with the axes of orthotropy:

$$f_{\mathrm{B}}(\boldsymbol{\sigma}) = \bar{a}|K_1 + K_2|^m + \bar{a}|K_1 - K_2|^m + (2-\bar{a})|2K_2|^m = 2\bar{\sigma}^m, \tag{3.32}$$

where $K_1 = \dfrac{\sigma_{11} + h\sigma_{22}}{2}$, $K_2 = \sqrt{\left(\dfrac{\sigma_{11} - h\sigma_{22}}{2}\right)^2 + p^2\sigma_{12}^2}$.

Coefficients $\bar{a}, h, p, \bar{\sigma}, m$ are material parameters established in experiments. For f.c.c. crystals the exponent $m = 8$ is suggested and for b.c.c crystals $m = 6$. The

function f_B is homogeneous of degree m. According to the authors, this yield condition agrees with the Taylor-Bishop-Hill yield surface [7, 8]. The last yield surface is specified by the microstructure of the polycrystalline aggregate.

Now we calculate a invariant form of the condition (3.32). Functions K_1 and K_2 we can express by the invariants of the plane stress tensor as follows:

$$K_1 = \frac{(1+h)\operatorname{tr}\boldsymbol{\sigma} + 2(1-h)\operatorname{tr}\mathbf{Ms}}{4}, \tag{3.33}$$

$$K_2 = \sqrt{\left(\frac{(1-h)\operatorname{tr}\boldsymbol{\sigma} + 2(1+h)\operatorname{tr}\mathbf{Ms}}{4}\right)^2 + \frac{p^2}{2}(\operatorname{tr}\mathbf{s}^2 - 2(\operatorname{tr}\mathbf{Ms})^2)}. \tag{3.34}$$

Substituting into these expressions the values of yield stresses obtained in the tests (3.20)-(3.21), we obtain the following equations defining material parameters:

$$\bar{\sigma} = Y, \qquad h = \frac{Y_1}{Y_2}, \qquad \text{for} \qquad h > 1: \tag{3.35}$$

$$\bar{a} = \frac{2Y_1^m - 2(h-1)^m Y_p^m}{Y_p^m[1 + h^m - (h-1)^m]}, \qquad p = \pm\left|\frac{2}{2\bar{a} + (2-\bar{a})2^m}\right|^{\frac{1}{m}} \frac{Y_1}{k}.$$

For the special cases of orthotropy we have

- for cubic symmetry:

$$h = 1 \Rightarrow K_1 = \frac{1}{2}\operatorname{tr}\boldsymbol{\sigma}, \quad K_2 = \sqrt{(\operatorname{tr}\mathbf{Ms})^2 + \frac{p^2}{2}(\operatorname{tr}\mathbf{s}^2 - 2(\operatorname{tr}\mathbf{Ms})^2)},$$

- for plane isotropy:

$$h = 1, \quad p = 1 \Rightarrow K_1 = \frac{1}{2}\operatorname{tr}\boldsymbol{\sigma}, \quad K_2 = \sqrt{\frac{1}{2}\operatorname{tr}\mathbf{s}^2} = \frac{1}{\sqrt{2}}\|\mathbf{s}\|, \tag{3.36}$$

where $\|\mathbf{s}\|$ denotes the norm of the stress deviator in a two-dimensional space.

To find the invariant form of the Barlat-Lian criterion using the stress invariants from the Eq. (3.5), we have to apply the expressions:

$$\operatorname{tr}\mathbf{Ms} = \operatorname{tr}\mathbf{M}\boldsymbol{\sigma} - \frac{1}{2}\operatorname{tr}\boldsymbol{\sigma}, \quad \operatorname{tr}\mathbf{s}^2 = \operatorname{tr}\boldsymbol{\sigma}^2 - \frac{1}{2}(\operatorname{tr}\boldsymbol{\sigma})^2. \tag{3.37}$$

As for the Hill yield condition, we outline now the tensile yield stress at the angle ϕ to the $\mathbf{m}_1$ axis:

$$\sigma_\phi = \bar{\sigma}\left(\frac{2}{\bar{a}|k_1^\phi + k_2^\phi|^m + \bar{a}|k_1^\phi - k_2^\phi|^m + (2-\bar{a})|2k_2^\phi|^m}\right)^{\frac{1}{m}}, \tag{3.38}$$

where

$$k_1^\phi = \frac{1}{2}(\cos\phi^2 + h\sin\phi^2),$$

$$k_2^\phi = \frac{1}{2}\sqrt{(\cos\phi^2 - h\sin\phi^2)^2 + p^2(\sin 2\phi)^2}.$$

Functions g_i from the general flow rule (3.9) for the case of the Barlat-Lian criterion take the form:

$$(3.39)\quad g_1 = f_1(\boldsymbol{\sigma})\frac{1+h}{4} + \frac{f_2(\boldsymbol{\sigma})}{4K_2}\left[\frac{1}{4}(1-h)^2\,\mathrm{tr}\,\boldsymbol{\sigma} + \frac{1}{2}(1-h^2)\mathrm{tr}\,\mathbf{Ms}\right],$$

$$(3.40)\quad g_2 = \frac{f_2(\boldsymbol{\sigma})}{4K_2}p^2,$$

$$(3.41)\quad g_3 = f_1(\boldsymbol{\sigma})\frac{1-h}{2} + \frac{f_2(\boldsymbol{\sigma})}{4K_2}\left[\frac{1}{2}(1-h^2)\mathrm{tr}\,\boldsymbol{\sigma} + [(1+h)^2 - 4p^2]\mathrm{tr}\,\mathbf{Ms}\right],$$

where

$$f_1(\boldsymbol{\sigma}) = \frac{\partial f_B}{\partial K_1} = \bar{a}m\left[|K_1{+}K_2|^{m-2}(K_1{+}K_2) + |K_1{-}K_2|^{m-2}(K_1{-}K_2)\right],$$

$$f_2(\boldsymbol{\sigma}) = \frac{\partial f_B}{\partial K_2} = \bar{a}m\left[|K_1{+}K_2|^{m-2}(K_1{+}K_2) - |K_1{-}K_2|^{m-2}(K_1{-}K_2)\right] + 2m(2{-}\bar{a})(2K_2)^{m-1}.$$

Using the flow rule we can find the expression which gives the Lankford coefficient R_ϕ. Thus

$$(3.42)\quad R_\phi = \frac{2f_1^\phi(\sin^2\phi^2 + h\cos^2\phi) + \frac{f_2^\phi}{k_2^\phi}\left[\frac{1}{4}\sin^2 2\phi[(1{+}h)^2 - 4p^2] - h\right]}{-[2(1{+}h)f_1^\phi + \frac{f_2^\phi}{k_2^\phi}(\cos^2\phi + \sin^2\phi h^2 - h)]}.$$

Functions f_1^ϕ and f_2^ϕ from the Eq. (3.42) are equal to $f_1(\mathbf{W}_\phi)$ and $f_2(\mathbf{W}_\phi)$, respectively.

The Eqs. (3.13),(3.14) or (3.15),(3.16) that describe the condition of strain localization are also applicable to the flow rule associated with the Barlat-Lian yield surface where the functions g_i are defined by (3.39)-(3.41).

3.2. The proposed yield surface for polycrystals

Polycrystal models based on the microstructure of the grain aggregate use the constitutive model of the single grain presented in the Sec. 2. Unlike phenomenological models, they allow to follow crystallographic texture development due to deformation process.

Starting-point of these theories are definitions of *a grain aggregate* and *a representative volume element*. As a *grain aggregate* we consider the set of grains which have identical elastic-plastic properties and differ only in crystallographic lattice orientation. As a *representative volume element* we consider the set of grains to which we can refer averaged macroscopic stress and strain measures. Usually we can assume that there are about 1000 grains in the material point at the macro-scale defined in such a way. These grains have diameters of about 100 μm [21].

One of the oldest computational models of this kind for polycrystals is the Sachs model proposed in 1928 [44]. It describes initial yielding of grain aggregates assuming that each grain in the representative volume element is subjected to the same stress state. In this model the condition of kinematic compatibility on the grain boundaries is not satisfied. The Taylor model from 1938 [45] assumes that the same macroscopic plastic strain rate is imposed on each grain. Using this assumption Taylor obtained the macroscopic yield stress in tension for the polycrystal. The condition of uniform deformation for the polycrystal element imposes strong constrains on the Taylor model. In this model the equilibrium equations for grain boundaries are not satisfied. There are also relaxed Taylor models which assume that only some components of the plastic strain rate tensor in the grain are equal to the components of the macroscopic plastic strain rate tensor.

By means of the Taylor assumption, Bishop and Hill searched in their works published in 1951 [7, 8] for the global yield surface of the polycrystal. On the level of the single grain they assumed the Schmid yield condition. In their calculation such a set of slip systems was active that minimized the total work done during slipping. To construct the global yield surface they used also the condition of convexity of the yield surface for the single grain and the Hill consistency condition for the global and local fields of stress and strains:

$$\dot{w} = \langle \boldsymbol{\sigma}^{\mathrm{g}} : (\mathbf{D}^{\mathrm{p}})^{\mathrm{g}} \rangle = \bar{\boldsymbol{\sigma}} : \bar{\mathbf{D}}^{\mathrm{p}},$$

where quantities $(\mathbf{D}^{\mathrm{p}})^{\mathrm{g}}$ and $\boldsymbol{\sigma}^{\mathrm{g}}$ denoted the local plastic strain rate tensor and the local Cauchy stress tensor in the grain g respectively, $\bar{\boldsymbol{\sigma}}$ and $\bar{\mathbf{D}}^{\mathbf{p}}$ – the global strain rate tensor and the global Cauchy stress tensor, $\langle . \rangle$ – averaging over the representative volume element, and $\dot{w}$ – the rate of plastic work. It is evident that $(\mathbf{D}^{\mathrm{p}})^{\mathrm{g}} = \bar{\mathbf{D}}^{\mathrm{p}}$ because of the Taylor assumption. The rate of plastic work can also be expressed as a product of the effective rate of plastic deformation $(D^{\mathrm{p}})^{\mathrm{eff}}$ and the effective stress σ^{eff} which is the strength measure of the material when the plastic flow begins:

$$\dot{w} = \sigma^{\mathrm{eff}} (D^{\mathrm{p}})^{\mathrm{eff}}.$$

Graphic interpretation of the effective stress σ^{eff} is presented in the Fig. 4. The yield surface $F(\bar{\sigma})$ is the inner envelope of all the hyperplanes Π orthogonal to the $\mathbf{D}^{\text{p}}$ direction for which the distance to the point $\bar{\sigma} = 0$ is equal to the effective stress σ^{eff}.

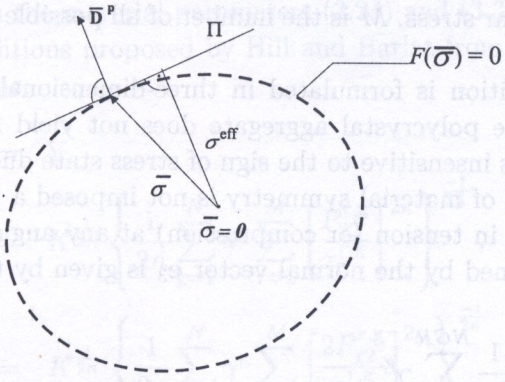

FIG. 4. Global yield surface for the polycrystal-construction.

The first *self-consistent* model for polycrystal (it satisfies the equilibrium equations as well as the condition of kinematic compatibility on the grain boundaries) was the Kröner model proposed in 1961 [36] and extended in the work [3]. It used the solution of the Eshelby problem for the spherical inclusion [14]. In this model, re-orientation of the grains during deformation process was not taken into account. Another self-consistent model was proposed by Hill in 1965 [24].

The general theory of constitutive models for the polycrystalline materials was also developed in [25] and [28, 29]

In this paper we propose the initial yield surface for polycrystals which is given by the formula (see also [13, 19, 35]):

$$\frac{1}{2n}\sum_{g=1}^{N}\gamma^{g}\sum_{r=1}^{M}\left[\frac{\bar{\sigma}:\mathbf{P}^{r,g}}{\tau_{c}^{r,g}}\right]^{2n} - K = 0, \tag{3.43}$$

where γ^{g} denotes the volume fraction (or probability of finding) of the grains with orientation g in the grain aggregate, and N is the total number of considered orientations. Quantity $\bar{\sigma}$ denotes the macroscopic stress tensor in the polycrystal. We assume that when the plastic flow begins, the stress state is uniform in the polycrystal element, so the Sachs assumption is satisfied. Parameter K is established in the experiment carried out on the macro-level, for example uniaxial tension in $\mathbf{e}_1$ direction, thus:

$$K = \frac{1}{2n}\sum_{g=1}^{N}\gamma^{g}\sum_{r=1}^{M}\left[\frac{YP_{11}^{r,g}}{\tau_{c}^{r,g}}\right]^{2n},$$

where $P_{11}^{r,g}$ is the component of the tensor $\mathbf{P}^{r,g}$ in the orthonormal basis $\{\mathbf{e}_i\}, i = 1,2,3$ joined with the sample, and Y is the initial yield stress. The quantities $\mathbf{P}^{r,g}$ and $\tau_c^{r,g}$ are defined as in the Sec. 2, so $\mathbf{P}^{r,g}$ is the symmetric part of the diad which defined the r-th slip system in the grain g, and $\tau_c^{r,g}$ denotes corresponding critical resolved shear stress. M is the number of all possible slip systems for the grain g.

This yield condition is formulated in three-dimensional space. It is worth mentioning that the polycrystal aggregate does not yield for any hydrostatic stress state and it is insensitive to the sign of stress state due to the form of the exponent. The kind of material symmetry is not imposed a priori.

The yield stress in tension (or compression) at any angle ϕ to the direction $\mathbf{e}_1$ in the plane defined by the normal vector $\mathbf{e}_3$ is given by the expression:

$$\sigma_\phi = \left[K \left(\frac{1}{2n} \sum_{g=1}^{NGR} \gamma^g \sum_{r=1}^{M} \left(\frac{P_{11}^{r,g} \cos^2\phi + P_{22}^{r,g} \sin^2\phi + P_{12}^{r,g} \sin 2\phi}{\tau_c^{r,g}} \right)^{2n} \right)^{-1} \right]^{\frac{1}{2n}}, \tag{3.44}$$

where the coefficients $P_{ij}^{r,g}$ are the components of the tensor $\mathbf{P}^{r,g}$ in the basis $\{\mathbf{e}_i\}$.

The following flow rule is associated with the yield condition (3.43):

$$\mathbf{D}^p = \lambda \sum_{g=1}^{N} \gamma^g \sum_{r=1}^{M} \frac{1}{\tau_c^{r,g}} \left[\frac{\bar{\boldsymbol{\sigma}} : \mathbf{P}^{r,g}}{\tau_c^{r,g}} \right]^{2n-1} \mathbf{P}^{r,g}. \tag{3.45}$$

Using the equation (3.45) we can find the Lankford coefficient:

$$R_\phi = \frac{D_{22}^\phi}{D_{33}^\phi}, \tag{3.46}$$

where for the proposed yield surface:

$$D_{22}^\phi = \sum_{g=1}^{N} \gamma^g \sum_{r=1}^{M} \frac{1}{\tau_c^{r,g}} \left[\frac{\tau_\phi^{r,g}}{\tau_c^{r,g}} \right]^{2n-1} \left(P_{11}^{r,g} \sin^2\phi + P_{22}^{r,g} \cos^2\phi - P_{12}^{r,g} \sin 2\phi \right),$$

$$D_{33}^\phi = \sum_{g=1}^{N} \gamma^g \sum_{r=1}^{M} \frac{1}{\tau_c^{r,g}} \left[\frac{\tau_\phi^{r,g}}{\tau_c^{r,g}} \right]^{2n-1} P_{33}^{r,g},$$

and

$$\tau_\phi^{r,g} = P_{11}^{r,g} \cos^2\phi + P_{22}^{r,g} \sin^2\phi + P_{12}^{r,g} \sin 2\phi.$$

In the next section we will compare the proposed yield surface with the Hill yield condition (3.17) and the Barlat-Lian yield condition (3.32). We will also compute plastic anisotropy development in the polycrystalline aggregate due to evolution of crystallographic texture in large deformation processes (see also [18]).We will obtain the material parameters (3.24) and (3.35) defining the phenomenological conditions proposed by Hill and Barlat from the criterion (3.43) using the expressions:

$$Y_1 = Y, \tag{3.47}$$

$$Y_2 = K^{\frac{1}{2n}} \left\{ \frac{1}{2n} \sum_{g=1}^{N} \gamma^g \sum_{r=1}^{M} \left[\frac{P_{22}^{r,g}}{\tau_c^{r,g}} \right]^{2n} \right\}^{\frac{-1}{2n}}, \tag{3.48}$$

$$k = K^{\frac{1}{2n}} \left\{ \frac{1}{2n} \sum_{g=1}^{N} \gamma^g \sum_{r=1}^{M} \left[\frac{2P_{12}^{r,g}}{\tau_c^{r,g}} \right]^{2n} \right\}^{\frac{-1}{2n}}, \tag{3.49}$$

$$Y_p = K^{\frac{1}{2n}} \left\{ \frac{1}{2n} \sum_{g=1}^{N} \gamma^g \sum_{r=1}^{M} \left[\frac{P_{11}^{r,g} + P_{22}^{r,g}}{\tau_c^{r,g}} \right]^{2n} \right\}^{\frac{-1}{2n}}. \tag{3.50}$$

In the above formulas $\mathbf{e}_3$ defines the considered plane, and $\mathbf{e}_1$ and $\mathbf{e}_2$ are assumed to be co-axial with the main directions of orthotropy $\mathbf{m}_1$ and $\mathbf{m}_2$ in this plane.

4. Comparison of the phenomenological yield surfaces with the proposed yield surface

In this section will we compare the shape of the phenomenological yield surfaces discussed in the Sec. 3.1 with the shape of the proposed yield surface given by the formula (3.43). In the beginning we will consider the case of plane isotropy. Later on we will focus on the evolution of anisotropy due to two specific large plastic deformation processes – the texture development in the sheet rolling and pure shear in the sheet plane. For these two cases we will assume that the sheet is plastically isotropic at the beginning of the process.

4.1. Plane isotropy

Now we will consider a sheet which is isotropic in its plane defined by the normal vector $\mathbf{e}_3$ and which can be anisotropic in its section orthogonal to the sheet plane (see Fig. 5). This kind of sheet symmetry is called plane isotropy.

If we use the Hill yield condition (3.17) to describe plastic flow of this sheet then this condition takes the form (3.26). In the case of the Barlat-Lian yield

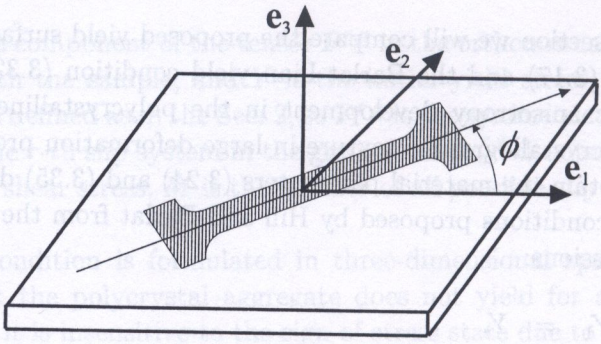

FIG. 5. Sheet geometry.

surface (3.18) we will use the form (3.36) of it. Note that, in order to describe behaviour of the material in both cases, we have to establish two material parameters: σ and τ for the Hill criterion, and $\bar{a}$ and $\bar{\sigma}$ for the Barlat-Lian criterion. These parameters are often expressed by the yield stresses obtained in uniaxial tension (3.22) and equi-biaxial tension (3.21):

$$\sigma = Y_p, \qquad \left(\frac{\sigma}{\tau}\right)^m = (2q)^m - 1, \qquad \bar{\sigma} = Y_1, \qquad \bar{a} = q^m,$$

where

$$q = \frac{Y_p}{Y_1}. \tag{4.1}$$

Because of the requirement of convexity for the yield surface, the following conditions imposed on the ratio q and the exponent m must be satisfied (see [26] and [5]):

$$q > 0.5 \quad \text{for the Hill condition,} \tag{4.2}$$

$$q^{-m} < 2 \quad \text{for the Barlat-Lian condition.} \tag{4.3}$$

Using the value of the Lankford coefficient R_ϕ we can evaluate anisotropy of the sheet in its cross-section. In the case of plane isotropy this coefficient has a constant value R and for the Hill condition it takes the form:

$$R_H = 2^{m-1}q^m - 1 \tag{4.4}$$

while for the Barlat-Lian surface:

$$R_B = 2q^m - 1. \tag{4.5}$$

Note that if the sheet is isotropic not only in its plane but also in its cross-sections, then in uniaxial tension, the change of thickness of the sample is the

same as the change of its width (see Fig. 5). The Lankford coefficient R is then equal to one. In the case of the Barlat-Lian condition it occurs when $q = 1$, and in the case of the Hill surface – when $q^m = 2^{2-m}$.

Let us call "*anomalous*" such behaviour that cannot be described by the quadratic yield condition proposed in 1948. In the case of "*anomalous*" behaviour, for the ratio $q < 1$ we obtain the Lankford coefficient $R > 1$ and for $q > 1$ - the Lankford coefficient $R < 1$. If we look at the expressions (4.4) and (4.5) we will find out that using the Hill condition, it is possible to describe such a behaviour for some range of the exponent m. It is impossible to describe such a behaviour by the Barlat-Lian yield surface.

In order to prevent the material from "*non-physical*" behaviour that means increasing of sample thickness or width during uniaxial tension, the Lankford coefficient has to be larger than zero for both the conditions. In the case of the Hill yield surface it imposes, apart from the inequality (4.2), additional condition on the ratio q and the exponent m:

$$q^m > 2^{1-m}. \tag{4.6}$$

For the Barlat-Lian yield condition the Lankford coefficient R is greater than zero if the inequality (4.3) is satisfied.

Stress states that satisfy the Eqs. (3.15) and (3.16) are essential for possible strain localization. In the case of plane isotropy and the Hill yield surface, these equations have the form:

$$|\operatorname{tr}\boldsymbol{\sigma}|^{m-2}\operatorname{tr}\boldsymbol{\sigma} = \pm[(2q)^m - 1](2\operatorname{tr}\mathbf{s}^2)^{\frac{m-1}{2}} \quad \text{or} \quad \operatorname{tr}\boldsymbol{\sigma} = 0 \tag{4.7}$$

and for the Barlat-Lian yield surface:

$$\left(\frac{|K_1 - K_2|}{2K_2}\right)^{m-1} = \frac{2-q^m}{q^m} \quad \text{or} \quad \left(\frac{|K_1 + K_2|}{2K_2}\right)^{m-1} = \frac{q^m - 2}{q^m} \quad \text{or} \quad K_1 = 0, \tag{4.8}$$

where functions K_1 and K_2 are described by the expressions (3.36). For the plane stress tensors which satisfy these equations, the associated flow rule predicts a plane strain state. In the case of the considered yield conditions, the Eq. (3.16) is satisfied by the equal stress states and it does not depend on the ratio q. It is apparent from this equation that for the plane stress deviator we have plane strain state in the sheet plane. Solutions of the Eq. (3.15) depend on q so they must also depend on R.

In conclusion we can emphasize that knowing the Lankford coefficient R from the experiments, we can propose the proper m value as well as the proper yield function f for observed plastic flow process.

Further we will compare the shape of the phenomenological yield surfaces proposed by Hill and Barlat and Lian with the yield surface given by the formula (3.43). Coefficient $q = 0.9984$ is computed from the Eqs. (3.47), (3.50) and (4.1) for $2n = 8$. Plane isotropy close to the full isotropy of the sheet is obtained by uniform distribution of 2000 orientations of the f.c.c. grains. The way in which the Euler angle space is divided in order to obtain uniform distribution of orientations can be found in [30] or [11]. For the Barlat-Lian yield condition $m = 8$ is assumed, and for the Hill yield criterion $m = 1.5$ is assumed. We also present the results obtained for the Hill yield condition where $m = 8$. The restrictions (4.2) and (4.6) imposed on the ratio q for the Hill yield surface are satisfied. As far as the Barlat-Lian yield condition is considered, inequality (4.3) gives the following limit for the q value:

$$q > 2^{-0.125}, \quad \text{where} \quad 2^{-0.125} \approx 0.917.$$

The coefficient q computed for 2000 grain orientations satisfies this condition. Note that this bottom limit for q value for $m = 8$ (recommended for f.c.c. crystals by Barlat) composes a rather strong restriction. For b.c.c. crystals ($m = 6$ is recommended by Barlat) this restriction is a bit weaker:

$$q > 2^{-1/6}, \quad \text{where} \quad 2^{-1/6} \approx 0.891.$$

In the Fig. 6 four cross-sections of the considered yield surfaces are presented. The best agreement is achieved between the proposed yield surface and the Barlat-Lian yield condition for all the presented cross-sections. In the case of the Hill yield condition for $m = 1.5$, good agreement with the proposed yield surface is obtained for $\sigma_{12} = 0$ and $\sigma_{11} = \sigma_{22}$ cross-sections, while the shape of the Hill yield surface differs significantly for the remaining cross-sections. In the last case this yield surface predicts greater value of yield stresses than the proposed yield surface. It is different for the Hill yield criterion for $m = 8$: $\sigma_{12} = 0$ and $\sigma_{11} = \sigma_{22}$ cross-sections differ here from those obtained for the other yield surfaces. Moreover, it is worth mentioning that the yield surface given by the formula (3.43) and the Barlat-Lian yield surface exhibit greater number of rounded corners. Those corners do not appear for any considered yield surfaces in the $\sigma_{22} = 0$ and $\sigma_{11} = -\sigma_{22}$ cross-sections.

The Eqs. (4.7) and (4.8) are solved in the cross-sections presented in the Fig. 6 in order to obtain such stress states for which strain localization is possible. Moreover, such a stress states are calculated for the yield condition (3.43) using the expressions (3.15) and (3.16) as well as the flow rule (3.45). The results are collected in the Table 1.

Due to similarity of the shape of the yield surface for the Barlat-Lian yield condition and the proposed yield condition (the Eq. (3.43)), the stress tensors

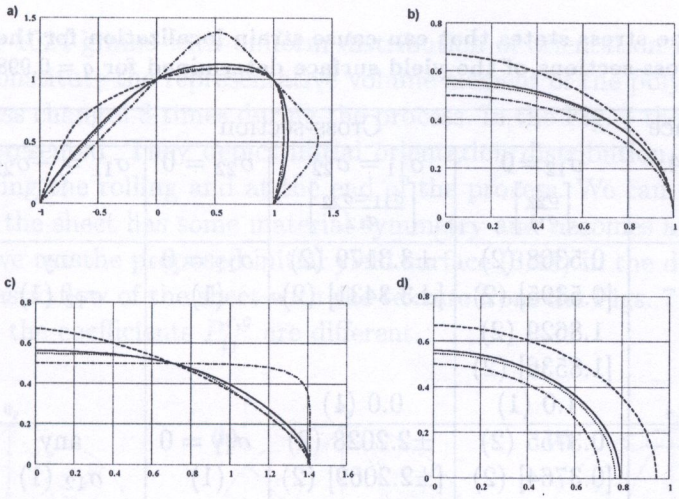

FIG. 6. Cross-sections of the analyzed yield conditions for plane isotropy where $q = 0.9984$: a) $\sigma_{12} = 0$ b) $\sigma_{22} = 0$ c) $\sigma_{11} = \sigma_{22}$ d) $\sigma_{11} = -\sigma_{22}$. All values are related to the yield stress Y_1. **Legend**: (———) – the yield surface given by the formula (3.43) where $2n = 8$; (.....) – the Barlat-Lian yield condition $m = 8$; (– – –) – the Hill yield condition where $m = 1.5$, (– . – .) – the Hill yield condition where $m = 8$.

that can cause strain localization for those conditions are the closest. Such stress states predicted by the Hill yield surface are significantly different. For all the considered yield conditions the Eq. (3.16) is satisfied for the same stress states in the case of plane isotropy.

It is worth looking at the results placed in the Table 1 that concern the Lankford coefficient R. Uniform distribution of grain orientations simulates full isortopy of the sheet but of course, it is only an approximation. In the table the average value of R is put for the proposed condition (3.43). This value is close but not equal to one. For the Barlat-Lian yield condition it is also close to one but as far as the Hill yield condition is concerned, a strong in-plane anisotropy is observed. "Anomalous" behaviour of the material is predicted for the Hill yield condition for $m = 8$. Moreover, the value of R suggests that the change of the sample thickness is very small in comparison with the change of the sample width in uniaxial tension. This is a rather artificial example. In the case of suggested value ($m < 2$), the Lankford coefficient R does not exhibit anomaly. However in this case the difference between the change of thickness and the change of width is greater than that for the proposed yield surface (3.43) and the Barlat-Lian yield surface.

4.2. Rolling texture

In this part, the evolution of plastic anisotropy due to development of rolling texture will be presented. Evolution of this crystallographic texture is computed

Table 1. The stress states that can cause strain localization for the considered cross-sections of the yield surface determined for $q = 0.9984$.

Yield surface $q = 0.9984$, [$q = 1$]	Cross-section				Value R
	$\sigma_{12}=0$ $\left[\frac{\sigma_{22}}{\sigma_{11}}\right]$	$\sigma_{11}=\sigma_{22}$ $\left[\frac{\sigma_{11}=\sigma_{22}}{\sigma_{12}}\right]$	$\sigma_{22}=0$	$\sigma_{11}=-\sigma_{22}$	
Hill $m = 1.5$	0.5368 (2) [0.5395] (2) 1.8629 (2) [1.8536] (2) -1.0 (1)	±3.3179 (2) [±3.3431] (2) 0.0 (1)	$\sigma_{11} = 0$ (1)	any σ_{12} (1)	0.4108 [0.4142]
Hill $m = 8$	0.3755 (2) [0.3764] (2) 2.6628 (2) [2.6571] (2) -1.0 (1)	±2.2028 (2) [±2.2069] (2) 0.0 (1)	$\sigma_{11} = 0$ (1)	any σ_{12} (1)	125.3 [127]
Barlat-Lian $m = 8$	0.4990 (2) [0.5] (2) 2.0038 (2) [2.0] (2) -1.0 (1)	±2.9925 (2) [±3.0] (2) 0.0 (1)	$\sigma_{11} = 0$ (1)	any σ_{12} (1)	0.9740 [1.0]
Barlat-Lian and Hill: $m = 2$	0.4984 (2) [0.5] (2) 2.0066 (2) [2.0] (2) -1.0 (1)	±2.9870 (2) [±3.0] (2) 0.0 (1)	$\sigma_{11} = 0$ (1)	any σ_{12} (1)	0.9935 [1.0]
The yield surface (3.43) $2n = 8$, 2000 grains	0.4913 (2) 2.0355 (2) -1.0 (1)	±2.9314 (2) 0.0 (1)	$\sigma_{11} = 0$ (1)	any σ_{12} (1)	~ 1.0561

Values in the square brackets correspond to $q = 1$.

(1) – the Eq. (3.16) is satisfied (it does not depend on q);

(2) – the Eq. (3.15) is satisfied.

by the numerical program using the constitutive model discussed in the Sec. 2. In this program, the crystallographic lattice re-orientation is calculated in every f.c.c. grain that build the polycrystalline aggregate. The calculations are performed for given velocity gradient $\mathbf{L^p}$ which is assumed to be the same for every grain. The direction of this tensor in the basis $\{\mathbf{e}_i\}$ (see Fig. 5) is specified as follows for rolling process:

$$\text{Path}(\mathbf{L^p}) = \text{Path}(\mathbf{D^p}) = \text{diag}[1.0, 0.0, -1.0].$$

There are 1024 grains with uniform distribution of orientation in the aggregate which constitute the representative volume element of the polycrystal. The sheet thickness changes 8 times during the process. In the Fig. 7 the pole figures <111> are presented. They depict initial orientation distribution, distribution obtained during the rolling and at the end of the process. We can observe that after rolling, the sheet has some material symmetry and becomes anisotropic in its plane. If we use the proposed initial yield surface (3.43) in the description of the initial plastic flow of the sheet with the texture from the Figs. 7 a, b, c, then in every case the coefficients $P_{ij}^{r,g}$ are different.

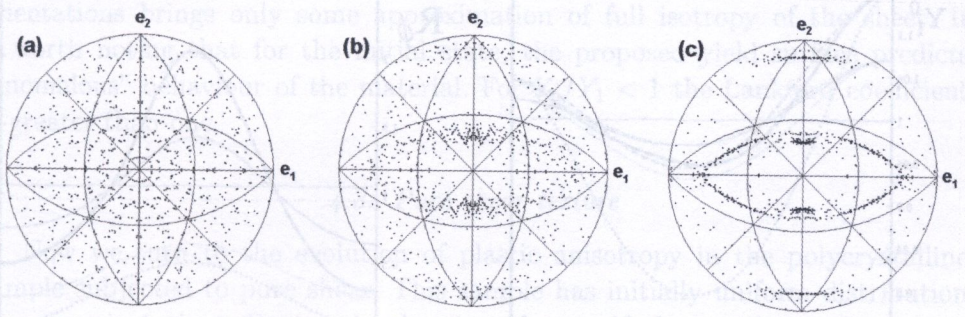

FIG. 7. Pole figures <111> for rolling process: the initial state (a), $t/t_0 = 0.25$ (b) and $t/t_0 = 0.5$ (c); t/t_0 denotes the ratio of the current sheet thickness to the initial sheet thickness.

The proposed yield condition ($2n = 8$) for those three textures is compared with the Barlat-Lian criterion ($m = 8$) and the Hill criterion ($m = 1.5$). In order to do this, the material parameters defining the phenomenological conditions are computed using the formulas (3.47)-(3.50). We assume as the main directions of orthotropy: $\mathbf{m}_1$ – the rolling direction, $\mathbf{m}_3$ – the direction normal to the sheet plane and $\mathbf{m}_2$ – the vector product of unit vectors $\mathbf{m}_1$ and $\mathbf{m}_3$. Thus, the main directions of orthotropy are in this case co-axial with the sample frame $\{\mathbf{e}_i\}$. Values of the material parameters obtained in this way are collected in the Table 2.

Values in the Table 2 indicate that the sheet has become orthotropic after rolling. Evolution of plastic anisotropy can be observed from the diagrams presenting the yield stress in tension (or compression) at any angle ϕ to the rolling direction and the Lankford coefficient R_ϕ (Fig. 8). The yield stress in tension σ_ϕ obtained for the Hill criterion (the formula (3.27)) is significantly different from the other conditions when the parameter b is calculated from the expression $(3.24)_2$. Therefore, in order to obtain this parameter, formula $(3.25)_2$ is used.

The revealed anisotropy in the yield stress in tension is not very strong for

Table 2. Material parameters obtained from the proposed yield surface (3.43) for crystallographic texture calculated for the specified range of rolling process.

Process range $\left[\frac{t}{t_0}\right]$	$\left[\frac{Y_1}{Y_1^0}\right]$	$\left[\frac{Y_2}{Y_1^0}\right]$	$\left[\frac{Y_p}{Y_1^0}\right]$	$\left[\frac{k}{Y_1^0}\right]$	$\left[\frac{Y_{45}}{Y_1^0}\right]$
1.0	1.0	1.0	0.999	0.559	1.0
0.5	1.071	1.023	0.984	0.534	0.972
0.125	1.148	1.046	0.998	0.510	0.947

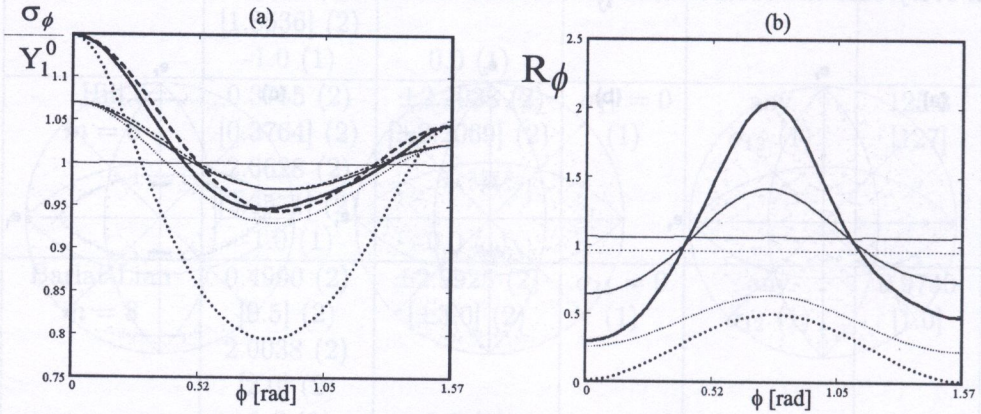

FIG. 8. Yield stress in uniaxial tension σ_ϕ/Y_1 (a) and the Lankford coefficient R_ϕ (b) **Legend**: (———) – yield surface given by the formula (3.43) where $2n = 8$; (.....) – Barlat yield condition where $m = 8$; (– – –) – Hill yield condition where $m = 1.5$. The increasing line thickness relates to the increasing range of rolling process.

all considered conditions. For the most advanced case of rolling texture it does not exceed 20%. The maximum value of the yield stress in tension is observed for the rolling direction, and the minimum value for $\phi = 45^o$ for all the presented yield conditions. Rolling process raises the yield stress in tension at the rolling direction and reduces for the angle $\phi = 45^o$. This statement is true for the proposed yield condition as well as for the phenomenological yield conditions.

Diagram of the Lankford coefficient R_ϕ, the formulas (3.31), (3.42) and (3.46), can give information about anisotropy of the plastic flow process. We observe here a significant difference between the behaviour of the material described by the yield surface given by the formula (3.43) and the one described by the phenomenological yield conditions proposed by Hill or Barlat and Lian. For the proposed yield surface there are such sample orientations given by the angle ϕ for which the sample width decreases more than the sample thickness ($R_\phi > 1$, strain localization by necking is predicted) and such sample orientations for which opposite behaviour is observed ($R_\phi < 1$, strain localization by thinning

is predicted). The Barlat-Lian surface as well as the Hill surface predict strain localization by thinning for all values of the angle ϕ. For the Barlat-Lian criterion, the minimum and the maximum value of the Lankford coefficient R_ϕ are close to each other and placed below one. For the proposed criterion, function R_ϕ increases rapidly in the region of $\phi = 22.5°$ to its maximum at $\phi = 45°$ and then decreases in the region of $\phi = 77.5°$. For these regions of the angle ϕ, small change in sample orientation can cause significant difference in the flow process. For the phenomenological yield conditions the function R_ϕ changes more smoothly. The initial value of the Lankford coefficient for the proposed yield surface (3.43) is slightly greater than one due to the fact that uniform distribution of grain orientations brings only some approximation of full isotropy of the sheet. It is worth noting that for the initial state, the proposed yield surface predicts "anomalous" behaviour of the material. For $Y_p/Y_1 < 1$ the Lankford coefficient is greater than one.

4.3. Pure shear texture

Now we turn to the evolution of plastic anisotropy in the polycrystalline sample subjected to pure shear. This sample has initially uniform distribution of grain orientations. During the shearing, the specified crystallographic texture develops in the sample. Texture development has been calculated for the velocity gradient $\mathbf{L^p}$, whose direction in the basis $\{\mathbf{e}_i\}$ (Fig. 5) could be expressed as follows:

$$\mathrm{Path}(L^{\mathrm{p}}_{12}) = \mathrm{Path}(L^{\mathrm{p}}_{21}) = 1.0.$$

Remaining components of the tensor $\mathbf{L^p}$ were equal to zero. Computational process has been conducted until the tangent of the shear angle θ became equal to 0.98. As for the rolling process, initial uniform distribution of grain orientations has been simulated by 1024 grains with different orientations. Computations have been made using the same constitutive model and the numerical program as for rolling process.

Texture development is presented in the Fig. 9 where the pole figures <111> are placed for the succeeding ranges of shearing process. It is observed that the lines representing directions <110> in the sample coordinate system $\{\mathbf{e}_i\}$ are the axes of symmetry for each pole figure. It is easy to see that these directions are also the principal axes of the tensor $\mathbf{D^p}$.

For the computed textures of pure shear, the change of the proposed yield surface as well as the change of the phenomenological yield conditions will be considered. Material parameters describing the shape of the Barlat-Lian surface and the Hill surface are calculated from the formulas (3.47)-(3.50) assuming that the principal directions of orthotropy $\{\mathbf{m}_\alpha\}, \alpha = 1, 2$ in the sheet plane are located at the angle

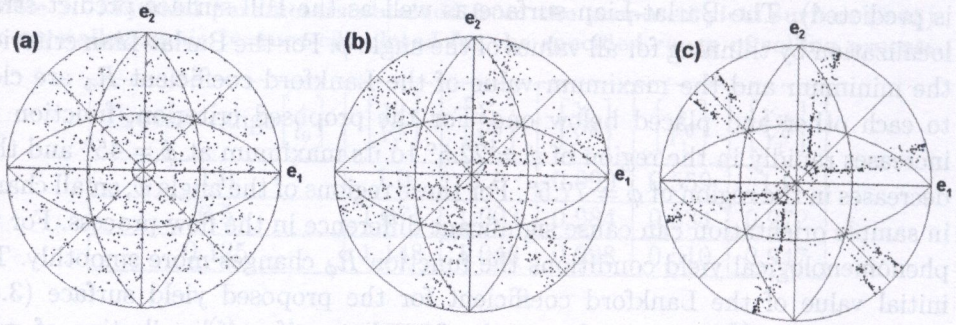

FIG. 9. Pole figures <111> for pure shear process: the initial state (a), $\tan(\theta) = 0.6$ (b) and $\tan(\theta) = 0.98$ (c)

45° to the sample axes $\{\mathbf{e}_\alpha\}$. This is indicated by the described symmetry of the pole figures. Calculated values of the material parameters are collected in the Table 3. As in the case of rolling process, in order to obtain the parameter b for the Hill condition, the expression (3.25) is used instead of (3.24).

Table 3. Material parameters obtained from the proposed yield surface (3.43) for the crystallographic texture calculated for the specified range of rolling process.

Process range $[\tan(\theta)]$	$\left[\frac{Y_1}{Y_1^0}\right]$	$\left[\frac{Y_2}{Y_1^0}\right]$	$\left[\frac{Y_p}{Y_1^0}\right]$	$\left[\frac{k}{Y_1^0}\right]$	$\left[\frac{Y_{45}}{Y_1^0}\right]$
0	1.0	1.0	0.999	0.559	1.0
0.6	1.067	0.988	1.021	0.548	0.992
0.98	1.158	0.997	1.046	0.545	0.997

Looking at the Table 3 we can see that the values of the yield stresses: Y_1 in tension in $\mathbf{m}_1$ direction and Y_p in equi-biaxial tension, increase while the yield stress k in pure shear decreases as the shear angle θ increases. Evolution of sheet anisotropy is easy to be observed in the Fig. 10, where diagrams of the yield stress in tension at orientation ϕ to the $\mathbf{m}_1$ axis and the Lankford coefficient R_ϕ are presented. The shape of these curves is different than for the rolling process, especially when the proposed yield surface (3.43) is concerned. We can observe in this case two local maxima of the function σ_ϕ: at the angle $\phi = 0°$ and $\phi \approx 60°$. For the other yield conditions one maximum of function σ_ϕ is found at the angle $\phi = 0°$, what means at the angle 45° to the $\mathbf{e}_1$ direction (see Fig. 5). Difference between the values of the yield stresses obtained for different angles ϕ do not exceed 15% for all the considered yield conditions.

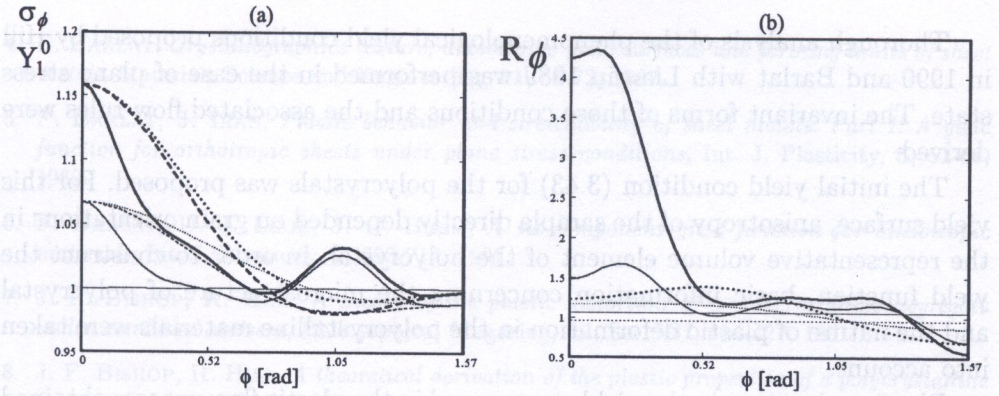

FIG. 10. Yield stress in uniaxial tension σ_ϕ/Y_1 (a) and the Lankford coefficient R_ϕ (b) **Legend**: (———) – yield surface given by the formula (3.43) where $2n = 8$; (.....) – Barlat yield condition where $m = 8$; (– – –) – Hill yield condition where $m = 1.5$. The increasing line thickness relates to the increasing range of shearing process.

The diagram of the Lankford coefficient R_ϕ shows that kinematical behaviour of the material strongly depends on the angle ϕ. For the sample orientation close to $\phi = 0°$ and $\phi = 60°$, the Lankford coefficient $R_\phi > 1$ and strain localization by necking is predicted. For $\phi = 45°$ and $\phi = 90°$ thinning is predicted. Such a behaviour of the material subjected to the pure shear process is predicted by the proposed texture-dependent yield surface. The function R_ϕ obtained for the Barlat-Lian yield surface with $m = 8$ is much more flat. In this case thinning is predicted for the angle ϕ between $0°$ and $\sim 60°$ and for the other values of the angle ϕ necking is predicted. As for the rolling textures, the Lankford coefficient R_ϕ calculated from the Hill yield condition for $m = 1.5$ significantly differs from the others. For any angle ϕ its value is less than one.

5. CONCLUSIONS

In the paper, the evolution of plastic anisotropy in the polycrystalline samples due to crystallographic texture development was presented. In order to describe the texture development, the rigid-plastic model with isotropic hardening was applied for the single grain. The regularized Schmid law proposed by Gambin was assumed as a yield condition for the single grain. In the processes associated with large plastic deformation, the crystallographic lattice re-orientation was computed for every grain in the polycrystalline aggregate. In these calculations the extended Clement formulas (2.12)-(2.16) appropriate for any grain orientation were used. This model was implemented in the numerical program used to calculate the texture development in the grain aggregate subjected to large deformation processes.

Thorough analysis of the phenomenological yield conditions proposed by Hill in 1990 and Barlat with Lian in 1989 was performed in the case of plane stress state. The invariant forms of those conditions and the associated flow rules were derived.

The initial yield condition (3.43) for the polycrystals was proposed. For this yield surface, anisotropy of the sample directly depended on grain orientations in the representative volume element of the polycrystal. In order to construct the yield function, basic information concerning the microstructure of polycrystal and the nature of plastic deformation in the polycrystalline materials were taken into account.

Plastic anisotropy in the yield stresses and in the plastic flow process obtained for the proposed yield surface was compared with the one obtained for the phenomenological yield conditions proposed by Hill and Barlat with Lian. Plastic anisotropy, which was analyzed, was caused by two large plastic deformation process: rolling and simple shear. For those two processes, the crystallographic texture development was computed by the numerical program described above. It was observed that as far as the yield stresses were concerned, the phenomenological yield surfaces and the proposed yield surface agreed quite well but as far as kinematical behaviour was concerned, they predicted different behaviours of the material. Those conditions predicted also different stress states that could cause strain localization.

Therefore one can conclude that a proper choice of the yield surface for given polycrystalline material should be based not only on the values of the yield stresses obtained in some experiments but also on the analysis of plastic flow process. For example, the value of the Lankford coefficient should be taken into account. It seems that the formula (3.12), which relates the yield stress in tension at the angle ϕ to orthotropy axis with the Lankford coefficient R_ϕ for any yield condition, can be helpful.

Development of plastic anisotropy in rolling and pure shear processes shows that even small change in the shape of yield surface can cause more significant changes of the principal directions of the strain rate tensor $\mathbf{D}^{\mathrm{p}}$. Those changes influence substantially the properties of the deformed metal element.

References

1. R. J. Asaro, *Crystal plasticity*, J. of Applied Mechanics, **50**, 921-934, 1983.

2. R. J. Asaro, *Micromechanics of crystals and polycrystals*, Advances in Applied Mechanics, **23**, 1983.

3. B. Budiansky, T. T. Wu, *Theoretical Prediction of plastic strains of polycrystals*, Proc. 4^{th} U.S. Nat. Congr. Appl. Mech., 1175-1185, ASME, New York 1962.

4. F. BARLAT, *Crystallographics texture, anisotropic yield surfaces and forming limits of sheet metals*, Materials Science and Engineering, **91**, 55-72, 1987.

5. F. BARLAT, J. LIAN, *Plastic behavior and stretchability of sheet metals. Part I: A yield function for orthotropic sheets under plane stress conditions*, Int. J. Plasticity, **5**, 51-66, 1989.

6. F. BARLAT, D. J. LEGE, J. C. BREM, *A six-component yield function for anisotropic materials*, Int. J. Plasticity, **7**, 693-712, 1991.

7. J. F. BISHOP, R. HILL, *A theory of the plastic distortion of a polycrystalline aggregate under combined stresses*, Philosophical Magazine, **42**, Ser. VII, 414-427, 1951.

8. J. F. BISHOP, R. HILL, *A theoretical derivation of the plastic properties of a polycrystalline face-centred metal*, Philosophical Magazine, **42**, Ser. VII, 1298-1307, 1951.

9. J. P. BOEHLER, *A simple derivation of representation for non-polynomial constitutive equations in some cases of anisotropy*, ZAMM, **59**, 157-167, 1979.

10. J. P. BOEHLER, *Applications of tensor functions in solid mechanics*, CISM Courses and Lectures, **292**, Springer-Verlag, Wien-New York 1987.

11. H. J. BUNGE, *Texture analysis in material science*, Mathematical Methods, London, Butterworths 1982.

12. A. CLEMENT, *Prediction of deformation texture using a physical principle of conservation*, Mater. Sci. Eng., **55**, 203-210, 1982.

13. M. DARRIEULAT, D. PIOT, *A method of generating analytical yield surfaces of crystalline materials*, Int. J. Plasticity, **12**, 5, 575-610, 1996.

14. J. D. ESHELBY, *The determination of the elastic field of an ellipsoidal inclusion and related problems*, Proc. Roy. Soc. London, **A241**, 376-296, 1957.

15. W. GAMBIN, *Crystal plasticity based on yield surface with rounded-off corners*, ZAMM, **71**, 4, T265-T268, 1991.

16. W. GAMBIN, *Plasticity of crystals with interacting slip systems*, Enging. Trans., **39**, 3-4, 303-324, 1991.

17. W. GAMBIN, *Refined analysis of elastic-plastic crystals*, Int. J. Solids Structures, **29**, 16, 2013-2021, 1992.

18. W. GAMBIN, F. BARLAT, *Modelling of deformation texture development based on rate independent crystal plasticity*, Int. J. Plasticity, **13**, 1/2, 75-85, 1997.

19. W. GAMBIN, K. KOWALCZYK, *Evolution of plastic anisotropy due to deformation texture development*, Mat. VII Inter. Symp. Plasticity'99, January 5-13, Mexico, Cancun 1999.

20. M. GOTOH, *A theory of plastic anisotropy based on a yield function of fourth order (plane stress state) - I/II*, Int. J. Mech. Sci., **19**, 505-512, 513-520, 1977.

21. K. S. HAVNER, *Finite Plastic deformation of crystalline solids*, Cambridge University Press, 1992.

22. R. HILL, *A theory of the yielding and plastic flow of anisotropic metals*, Proc. Roy. Soc., London, Ser.A, **193**, 281-297, 1948.

23. R. HILL, *Mathematical theory of plasticity*, Oxford, Clarendon Press, 1950.

24. R. HILL, *Continuum micro-mechanics of elastoplastic polycrystals*, J. Mech. Phys. Solids, **13**, 89-101, 1965.

25. R. HILL, *The essential structure of constitutive laws for metal composites and polycrystals*, J. Mech. Phys. Solids, **15**, 79-95, 1967.

26. R. HILL, *Theoretical plasticity of textured aggregates*, Math. Proc. Camb. Phil. Soc., **85**, 179-191, 1979.

27. R. HILL, *Constitutive modelling of orthotropic plasticity in sheet metals*, J. Mech. Phys. Solids, **38**, 3, 405-417, 1990.

28. R. HILL, J. R. RICE, *Constitutive analysis of elastic-plastic crystals at arbitrary strain*, J. Mech. Phys. Solids, **20**, 401-413, 1972.

29. R. HILL, J. R. RICE, *Elastic potential and the structure of inelastic constitutive laws*, SIAM J. Appl. Math., **25**, 3, 1973.

30. R. W. K. HONEYCOMB, *The plastic deformation of metals*, E. Arnold Ltd, 1984.

31. D. HULL, *Introduction to dislocations*, Pergamon Press, Oxford, 1984.

32. S. JEMIOŁO, J. J. TELEGA, *Representations of tensor functions and applications in continuum mechanics*, Prace IPPT, Warszawa, 3/1997.

33. S. JEMIOŁO, K. KOWALCZYK, *Invariant formulation and spectral decomposition of the Hill anisotropic yield criterion*, (in Polish), Prace Naukowe PW, Budownictwo, z. 133, 87-123, 1999.

34. U. F. KOCKS, *Constitutive behaviour based on crystal plasticity*, Reprinted from United Constitutive Equations for Creep and Plasticity, A.K. MILLER [Ed.], Elsevier 1987.

35. K. KOWALCZYK, W. GAMBIN, *Evolution of yield surface due to texture development*, Volume of abstracts, 33^{rd} Solid Mechanics Conference, Zakopane, September 5-9, 2000.

36. E. KRÖNER, *Zur plastischen Verformung des Vielkristalls*, Acta Met., **9**, 155-161, 1961.

37. E. H. LEE, *Elastic-plastic deformation at finite strains*, J. Appl. Mech., **36**, 1, 1969.

38. J. LIAN, F. BARLAT, B. BAUDELET, *Plastic behaviour and strechability of sheet metals. Part II: Effect of yield surface shape on sheet forming limit*, Int. J. Plasticity, **5**, 131-147, 1989.

39. R. MISES, *Mechanik der plastischen Formänderung von Kristallen*, Zeitschrift für Angewandte Mathematik und Mechanik, **8**, 161, 1928.

40. W. OLSZAK, W. URBANOWSKI, *The plastic potential and generalized distorsion energy in the theory of non-homogeneous anisotropic elastic-plastic bodies*, Arch. Mech. Stos., **8**, 4, 671-694, 1956.

41. W. OLSZAK, J. OSTROWSKA-MACIEJEWSKA, *The plastic potential in the theory of anisotropic elastic-plastic solids*, Engng. Fracture Mech., **21**, 4, 625-632, 1985.

42. J. OSTROWSKA-MACIEJEWSKA, *Mechanics of deformable bodies* [in Polish], PWN, Warszawa 1994.

43. J. RYCHLEWSKI, *Elastic energy decomposition and limit criteria* (in Russian), Advances in Mechanics, **7**, 3, 1984.

44. G. SACHS, *Zur Ableitung einer Fliessbedingung*, Zeichschrift des Vereins deutcher Ingenieure, **72**, 734, 1928.

45. G. I. Taylor, *Plastic strain in metals*, Journal of Institute of Metals, **62**, 307-324, 1938.

46. C. Teodosiu, J. L. Raphanel, L. Tabourot, *Finite element simulation of large elasto-plastic deformation in multicrystals*, MECAMAT'91, Theodosiu, Raphanel & Sidoroff [Ed.], Balkema, Rotterdam 1993.

Received July 19, 2000.